# Nitrite complexes of the rare earth elements

Jacky Pouessel, Pierre Thuéry, Jean-Claude Berthet, Thibault Cantat

Dalton Transactions

PAPER

View Article Online
View Journal | View Issue

# Nitrite complexes of the rare earth elements†

Cite this: *Dalton Trans.*, 2014, **43**, 4415

Received 27th September 2013,
Accepted 9th November 2013

DOI: 10.1039/c3dt52703d

www.rsc.org/dalton

Jacky Pouessel, Pierre Thuéry, Jean-Claude Berthet and Thibault Cantat*

The coordination chemistry of the nitrite anion has been investigated with rare earth elements, and the resulting complexes were structurally characterized. Among them, the first homoleptic examples of nitrite complexes of samarium, ytterbium and yttrium are described. The coordination behavior of the nitrite ion is directly controlled by the ionic radius of the metal cation. While the nitrito ligand is stable in the coordination sphere of cerium(III), it is readily reduced by $SmI_2$.



Nitrogen oxides are privileged ligands in the inorganic chemistry of the actinides and the rare earth elements (REEs), with nitric media being utilized at both ends of the life cycle of these strategic metal ions. In fact, the extraction of uranium or the REEs relies on the dissolution of f-element oxides and hydroxides in nitric acid.[1] Similarly, most technologies aimed at reprocessing nuclear waste or recycling the REEs involve the formation of nitrate complexes, prior to the separation of the effluent constituents.[1,2] Importantly, the nitrate anion ($NO_3^-$) exhibits a very rich redox chemistry and its problematic reduction to nitrite ($NO_2^-$) in natural groundwater and nuclear wastes motivated our preliminary interest in actinide nitrite complexes.[3,4] To overcome the absence of molecular models of thorium and uranium nitrite complexes, we reported, earlier this year, the synthesis of $[PPh_4]_2[Th(NO_2)_6]$ and $[PPh_4]_2[UO_2(NO_2)_4]$.[4] These complexes represent the first homoleptic complexes of uranyl and thorium with nitrite ligands. Beyond the nuclear fuel cycle context, lanthanide nitrites are desirable complexes both from structural and synthetic perspectives. Examples of nitrite complexes remain scarce within the REEs series. Early efforts focused on hexanitritolanthanide salts $Cs_2NaLn(NO_2)_6$ (Ln = La to Gd), which are obtained as solids from multi-step salt metathesis reactions in water.[5] This series was completed in 2004 with the isolation of $La(NO_2)_3$, as a coordination polymer.[6] Only six molecular nitrite complexes have been reported with REEs, namely $[(Tp^{Me2,4\text{-}Et})_2Sm(NO_2)]$,[7] $[(C_5H_5)_2Yb(NO_2)(THF)]$,[8] $[Ln(L)(NO_2)(H_2O)]$ (Ln = Sm, Eu, L = 2,2′-(biphenyl-4,4′-diylbis(oxy))diacetate),[9] $[La(NO_2)(SO_4)(H_2O)]$[10] and $[\{Fe(bipy)(CN)_4\}\cdot\{Sm(phen)(NO_2)(H_2O)_2\}]$.[11] Importantly, $[(C_5H_5)_2Yb(NO_2)(THF)]$ is the only complex obtained using a nitrite anion ($NaNO_2$) as a source of the nitrito ligand and the remaining examples resulted from redox disproportionation of nitrate or NO.[8] $[(Tp^{Me2,4\text{-}Et})_2Sm^{III}(NO_2)]$ was formed by reduction of NO to $NO_2^-$ and $N_2O$, promoted by $[(Tp^{Me2,4\text{-}Et})_2Sm^{II}]$.[7] Reduction of $NO_3^-$ to $NO_2^-$ was proposed as the source of the nitrito ligand in $[La(NO_2)(SO_4)(H_2O)]$.[10] From a structural point of view, the rational synthesis and the characterization of well-defined REEs nitrite complexes would therefore afford molecular models to better apprehend the redox chemistry of nitrogen oxides in lanthanide chemistry. Additionally, it has been recently shown that the nitrite anion $NO_2^-$ behaves as an attractive one electron oxidant in the coordination sphere of uranium(III) and uranium(IV), to access uranium–oxo functionalities.[4,12] The transposition of this chemical behavior to the lanthanide series could in principle offer an attractive route to Ln=O complexes or oxide clusters. Because the nitrite anion $NO_2^-$ possesses three donor atoms, it exhibits a variety of coordination behaviors and electron rich metal ions tend to form nitro complexes ($\kappa^1$-(*N*)-$NO_2$) while hard Lewis acids adopt the $\kappa^1$-(*O*)-$NO_2$ and $\kappa^2$-(*O*,*O*)-$NO_2$ coordination modes (nitrito ligand).[13] This coordination versatility has been recently utilized to prepare Ru/Ln heterometallic clusters, in the search for bifunctional materials combining photochromic and magnetic properties.[14] In the absence of isolated anionic nitritolanthanide complexes, the synthesis of such molecules is however limited to the formation of $\{Ln[Ru(NO)(\mu\text{-}NO_2)_4(\mu_3\text{-}OH)]_2Ln\}$ motifs, obtained from $Na_2[Ru(NO)(NO_2)_4OH]$ as a nitrite source.[14] From a synthetic viewpoint, the availability of well-defined REEs anionic nitrite complexes will allow the rapid construction of a wide range of heterometallic coordination polymers. In this contribution, we report novel nitrite compounds of the REEs (La, Ce, Pr, Nd, Sm, Yb, Y), including the first homoleptic examples of nitrite complexes of samarium, ytterbium and yttrium, from simple salt metathesis reactions between rare earth iodide and triflate salts with the nitrite anion. Importantly, all the nitrite compounds presented thereafter were characterized by X-ray diffraction.

*CEA, IRAMIS, SIS2M, CNRS UMR 3299, CEA/Saclay, 91191 Gif-sur-Yvette, France. E-mail: thibault.cantat@cea.fr; Fax: +33 1 6908 6640; Tel: +33 1 6908 4338*

†CCDC 963095–963108. For crystallographic data in CIF or other electronic format see DOI: 10.1039/c3dt52703d

$$Ln(OTf)_3 + 6\,[PPh_4][NO_2] \xrightarrow[-\,[PPh_4][NO_2]\;-\,3\,[PPh_4][OTf]]{\text{pyridine}} [PPh_4]_2[Ln(\kappa^2\text{-}NO_2)_5(py)]\;([PPh_4]_2[\mathbf{1}]\;(La),\;[PPh_4]_2[\mathbf{2}]\;(Ce)) \quad (1)$$

$$CeI_3 + 2\,[PPh_4][NO_2] + 3\,AgNO_2 \xrightarrow[-\,3\,AgI]{\text{pyridine}} [PPh_4]_2[\mathbf{2}] \quad (2)$$

$$CeI_3 + 3\,[PPh_4][NO_2] + 3\,AgNO_2 \xrightarrow[-\,[PPh_4][I]\;-\,2\,AgI]{\text{pyridine}} [PPh_4]_2[Ce(\kappa^2\text{-}NO_2)_5(\kappa^1\text{-}NO_2)Ag(py)_2]\;([PPh_4]_2[\mathbf{3}]) \quad (3)$$

$$[PPh_4]_2[\mathbf{2}] + AgNO_2 \xrightarrow{\text{pyridine}} [PPh_4]_2[\mathbf{3}] \quad (4)$$

**Scheme 1** Syntheses of $[PPh_4]_2$[**1**], $[PPh_4]_2$[**2**] and $[PPh_4]_2$[**3**] by salt metathesis reactions, carried out at RT in pyridine solvent.

We found in a previous study that $[PPh_4][NO_2]$ is a convenient source of nitrite to access homoleptic nitritoactinide complexes, as it is soluble in organic solvents and features a cation with a low Lewis acidity.[4] Addition of 6 equiv. $[PPh_4][NO_2]$ salt to a pyridine solution of $La(OTf)_3$ resulted in the deposition of light yellow crystals of complex $[PPh_4]_2[La(\kappa^2\text{-}NO_2)_5(py)]$ ($[PPh_4]_2$[**1**]), upon subsequent addition of $Et_2O$ (eqn (1) in Scheme 1). Utilizing $Ce(OTf)_3$, complex $[PPh_4]_2[Ce(\kappa^2\text{-}NO_2)_5(py)]$ ($[PPh_4]_2$[**2**]) was obtained in similar conditions. The structures of $[PPh_4]_2$[**1**] and $[PPh_4]_2$[**2**] were determined by X-ray diffraction analysis and the two complexes are isomorphous. Significant structural parameters are gathered in Table 1, for all the nitrito complexes obtained in this study, and the trends along the series of the REEs is discussed thereafter. As illustrated in Fig. 1 (see structure CCDC 963095 for $[PPh_4]_2$[**1**]), $[PPh_4]_2$[**2**] is a pentanitrito cerium(III) dianionic complex and the five nitrito ligands adopt the $\kappa^2$-(*O*,*O*)-$NO_2$ coordination mode. As a consequence, the $Ce^{3+}$ ion possesses a coordination number of 11, its coordination sphere being completed with a pyridine molecule. The resulting distorted all-faced capped trigonal prism geometry is more easily described by the spatial arrangement of the $CeN_6$ backbone, which represents an octahedron (Fig. 1). Of interest is the variation in the Ln–O and Ln–N distances in $[PPh_4]_2$[**1**] and $[PPh_4]_2$[**2**] which only reflects the difference in the metal ionic radii. Interestingly, the lanthanum dianion $\mathbf{1}^{2-}$ is isostructural to the nitrate complex $[La(\kappa^2\text{-}NO_2)_5(4,4'\text{-bipyH})]^{2-}$ and both complexes share similar structural parameters, namely a mean La–O [La–N] bond length of 2.64(5) [2.796(6)] Å *vs.* 2.63(3) [2.77] Å in the nitrito and nitrato complexes, respectively.[15] A similar trend was observed in the actinide series with $Th^{4+}$ and $UO_2^{2+}$ ions.[4,16,17] Synthetically, the difficult separation of $[PPh_4][OTf]$ from $[PPh_4]_2$[**X**] (**X** = **1**, **2**) urged us to develop a high yielding procedure to isolate analytically pure samples of these new complexes. The combination of $CeI_3$ and a 2 : 3 mixture of $[PPh_4][NO_2]$ and $AgNO_2$ in pyridine enables the quantitative formation of $[PPh_4]_2$[**2**], with AgI salt as the sole by-product (eqn (2)). $[PPh_4]_2$[**2**] is soluble in acetonitrile, while AgI readily precipitates in this solvent, enabling a simple separation of the reaction products. Following this synthetic route, $[PPh_4]_2$[**2**] was isolated in >92% yield as a pure solid, satisfactorily characterized by H,C,N elemental analyses.

Noticeably, while $Ce(NO_3)_6^{3-}$ complexes are classic in cerium(III) nitrate chemistry and nitrito and nitrato ligands share analogous coordination behaviors, the pentanitrito complex $\mathbf{2}^{2-}$ is the only cerium complex obtained in the presence of an excess $[PPh_4][NO_2]$. This result also contrasts with the stoichiometry in the solid hexanitritocerium salt $Cs_2NaCe(NO_2)_6$. This observation likely results from a stronger interligand electrostatic repulsion with the reduced $NO_2^-$ anion (compared to $NO_3^-$) and from the absence of Lewis acid countercation able to counterbalance this electrostatic repulsion in $[PPh_4]_2$[**2**] (compared to $Cs_2NaCe(NO_2)_6$). Nonetheless, as depicted in eqn (3), the hexanitrito complex $[PPh_4]_2$[**3**] can be formed selectively, from $CeI_3$ and a 3 : 3 mixture of $[PPh_4][NO_2]$ and $AgNO_2$. The X-ray diffraction structure of dianion $\mathbf{3}^{2-}$ is depicted in Fig. 2. Complex $[PPh_4]_2$[**3**] formally results from the displacement of the pyridine ligand in $[PPh_4]_2$[**2**] by an $[Ag(py)_2(\kappa^2\text{-}(O,O)\text{-}NO_2)]$ unit, $\kappa^1$-(*O*)-coordinated to the $Ce^{3+}$ ion, and $[PPh_4]_2$[**2**] can be converted to $[PPh_4]_2$[**3**] in the presence of $AgNO_2$, in >97% isolated yield (eqn (4)). Structurally, the Ce–O bond length of 2.526(4) Å for the bridging nitrite ligand is somewhat shorter than the mean Ce–O distance of 2.65(3) Å (range 2.596(4)–2.704(5) Å) for the $\kappa^2$-(*O*,*O*)-$NO_2$ ligands (2.60(4) Å in $[PPh_4]_2$[**2**]).

The coordination chemistry of the nitrite anion was then explored with smaller trivalent lanthanide ions, namely $Pr^{3+}$ and $Nd^{3+}$. $Pr(OTf)_3$ displays a reaction chemistry similar to $Ce(OTf)_3$ and it was converted to $[PPh_4]_2$[**4**], in the presence of 6 equiv. $[PPh_4][NO_2]$ (eqn (5) in Scheme 2). $[PPh_4]_2$[**4**] is isomorphous to $[PPh_4]_2$[**2**] and can be prepared from $PrI_3$, similarly to its La and Ce analogues (eqn (7)). In contrast, the metathesis reaction between $Nd(OTf)_3$ and 6 equiv. $[PPh_4][NO_2]$ afforded colourless crystals of a new neodymium nitrite complex, $[PPh_4]_2[Nd(\kappa^2\text{-}NO_2)_4(py)_2][NO_2]$ ($[PPh_4]_2$[**5**][$NO_2$]). The crystal structure of $[PPh_4]_2$[**5**][$NO_2$] reveals the co-crystallization of two salts, $[PPh_4]$[**5**] and $[PPh_4][NO_2]$. Interestingly, anion $\mathbf{5}^-$ presents a $Nd^{3+}$ cation stabilized by four $\kappa^2$-(*O*,*O*)-$NO_2$ and two pyridine ligands. With a coordination number of 10, the metal atom lies in the center of a bicapped square antiprism in which the two pyridine molecules serve as capping ligands (Fig. 3). Nonetheless, the formation of a pentanitrito complex of neodymium is synthetically available and two distinct complexes were successfully crystallized from a crude 1 : 2 : 3 mixture of $NdI_3$, $[PPh_4][NO_2]$ and $AgNO_2$, namely $[PPh_4]_2[Nd(\kappa^2\text{-}NO_2)_5(py)]$ ($[PPh_4]_2$[**6**]) and $[PPh_4]_2[Nd(\kappa^2\text{-}NO_2)_4(\kappa^1\text{-}NO_2)(py)]$ ($[PPh_4]_2$[**7**]). While $[PPh_4]_2$[**6**] is isomorphous to $[PPh_4]_2$[**X**] (**X** = **1**, **2**, **4**), anion $\mathbf{7}^{2-}$ formally results from the replacement of one pyridine molecule in $\mathbf{5}^-$ by a $\kappa^1$-(*O*)-$NO_2$ ligand (Fig. 4). As expected, the Nd–O bond length is shorter for the $\kappa^1$-(*O*)-$NO_2$ ligand (2.3896(16) Å) compared to the $\kappa^2$-(*O*,*O*)-$NO_2$ ligands (av. 2.58(4) Å) and complexes $\mathbf{6}^{2-}$ and $\mathbf{7}^{2-}$ exhibit similar bond distances (see Table 1). From a synthetic point of view, the purification procedure described for cerium salt $[PPh_4]_2$[**2**] (eqn (2) in Scheme 1) leads to the efficient isolation of $[PPh_4]_2$[**7**] in 94% yield, as an analytically pure solid (see the Experimental section). As exemplified with cerium complex $[PPh_4]_2$[**3**], the formation of hexanitrito complexes is

 

**Table 1** Selected bond lengths (Å) and angles (°)[a]

| | $[PPh_4]_2$[**1**] La | $[PPh_4]_2$[**2**] Ce | $[PPh_4]_2$[**3**] Ce | $[PPh_4]_2$[**4**] Pr | $[PPh_4]_2$[**5**][$NO_2$] Nd | $[PPh_4]_2$[**6**] Nd | $[PPh_4]_2$[**7**] Nd |
|---|---|---|---|---|---|---|---|
| M–O($\kappa^1$) | | | 2.526(4) | | | | 2.3896(16) |
| M–O($\kappa^2$) | 2.556(7)–2.727(11) [2.64(5)] | 2.545(8)–2.664(7) [2.60(4)] | 2.596(4)–2.704(5) [2.65(3)] | 2.524(9)–2.659(6) [2.59(4)] | 2.499(3)–2.606(3) [2.55(4)] | 2.530(3)–2.646(3) [2.58(3)] | 2.5421(15)–2.6480(14) [2.58(4)] |
| M–N(py) | 2.796(6) | 2.781(6) | | 2.764(5) | 2.6547(17), 2.6373(16) | 2.743(3) | 2.7081(15) |
| O–N($\kappa^1$) | | | 1.251(5), 1.244(6) | | | | 1.064(11)–1.290(14) [1.19(8)] |
| O–N($\kappa^2$) | 1.152(10)–1.266(9) [1.23(3)] | 1.161(9)–1.268(7) [1.23(3)] | 1.209(8)–1.316(8) [1.25(2)] | 1.178(9)–1.276(9) [1.24(3)] | 1.214(5)–1.282(6) [1.25(2)] | 1.210(4)–1.333(6) [1.25(3)] | 1.256(2)–1.273(2) [1.262(6)] |
| O–M–O($\kappa^2$) | 43.2(2)–47.17(19) [45.2(14)] | 44.2(2)–47.5(2) [46.1(13)] | 42.67(18)–46.80(13) [45.8(16)] | 45.3(2)–48.98(19) [46.9(13)] | 47.06(8)–48.81(10) [48.1(7)] | 43.72(15)–50.73(10) [47(2)] | 47.47(4)–48.79(5) [48.2(6)] |
| O–N–O($\kappa^1$) | | | 114.3(4) | | | | 121.6(4), 124.9(13) |
| O–N–O($\kappa^2$) | 105.1(9)–113.0(6) [111(3)] | 106.3(8)–114.0(10) [112(3)] | 105.4(8)–114.0(4) [111(3)] | 108.4(7)–114.6(9) [112(2)] | 109.6(4)–116.2(4) [113(2)] | 99.3(7)–114.9(5) [111(5)] | 112.67(17)–113.05(18) [112.9(2)] |

| | $[PPh_4]_2$[**8**] Pr | $[PPh_4]_2$[**9**] Nd | $[PPh_4]_2$[**10**]·py Sm | $[PPh_4]_2$[**11**]·py Yb | $[PPh_4]_2$[**12**]·py Y | $[PPh_4]_2$[**13**] Sm | $[PPh_4]_2$[**14**] Y |
|---|---|---|---|---|---|---|---|
| M–O($\kappa^1$) | 2.435(4), 2.438(4) | 2.425(3), 2.431(3) | | | | 2.3569(18)–2.4040(17) [2.38(2)] | 2.3005(15)–2.3410(15) [2.32(2)] |
| M–O($\kappa^2$) | 2.537(4)–2.662(4) [2.60(4)] | 2.519(3)–2.643(4) [2.58(4)] | 2.480(2)–2.558(2) [2.51(2)] | 2.3741(14)–2.5104(14) [2.42(4)] | 2.4191(14)–2.5226(14) [2.45(3)] | 2.5112(16)–2.5539(16) [2.54(2)] | 2.4424(13)–2.4929(14) [2.48(2)] |
| M–N(py) | | | | | | | |
| O–N($\kappa^1$) | 1.133(4), 1.185(4) | 1.130(4), 1.183(3) | | | | 1.091(3)–1.291(2) [1.20(7)] | 1.135(3)–1.292(2) [1.21(6)] |
| O–N($\kappa^2$) | 1.239(5)–1.280(5) [1.26(2)] | 1.242(5)–1.283(4) [1.257(14)] | 1.245(4)–1.274(3) [1.261(9)] | 1.246(3)–1.273(2) [1.262(8)] | 1.249(2)–1.273(2) [1.262(7)] | 1.247(3)–1.261(2) [1.255(6)] | 1.251(2)–1.270(2) [1.259(7)] |
| O–M–O($\kappa^2$) | 46.50(13)–48.85(13) [47.7(9)] | 46.92(12)–49.35(12) [48.1(9)] | 48.89(9)–50.18(7) [49.4(5)] | 50.76(5)–52.02(5) [51.2(5)] | 50.28(5)–51.37(5) [50.7(4)] | 48.30(5)–49.08(5) [48.7(4)] | 49.53(5)–50.44(5) [50.0(5)] |
| O–N–O($\kappa^1$) | 152.2(5), 151.7(4) | 152.6(5), 151.1(4) | | | | 114.58(18)–138.4(4) [123(13)] | 114.39(15)–134.2(3) [121(9)] |
| O–N–O($\kappa^2$) | 111.5(3)–115.2(3) [113.7(14)] | 111.6(3)–115.7(3) [113.9(15)] | 112.3(2)–113.7(2) [112.9(6)] | 111.68(17)–112.58(17) [112.3(4)] | 112.34(16)–113.01(17) [112.7(3)] | 112.81(18)–113.61(19) [113.1(4)] | 112.30(16)–112.58(15) [112.46(12)] |

[a] Individual values or ranges are given, with average values in brackets in the last case.

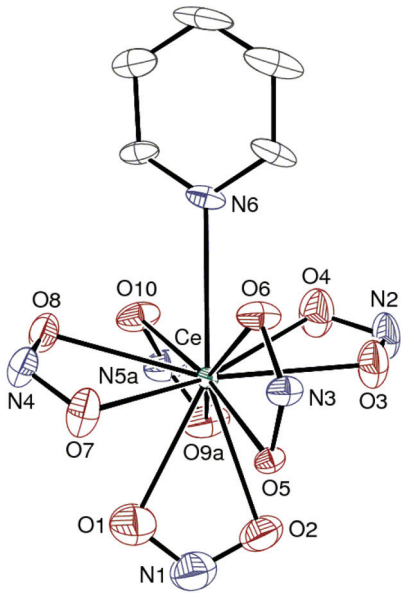


**Fig. 1** Molecular structure of anion $\mathbf{2}^{2-}$ with displacement ellipsoids drawn at the 20% probability level. Only one position of the disordered atoms is represented.

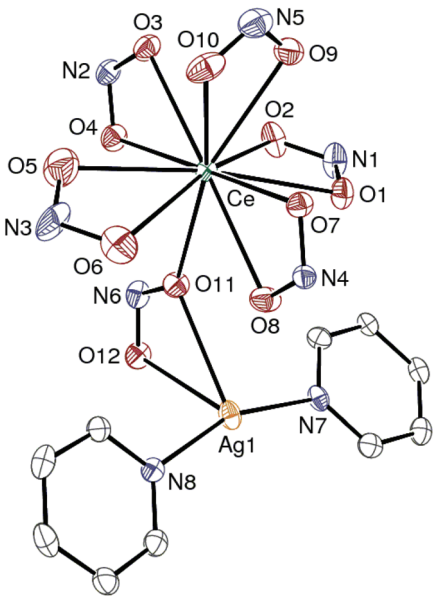


**Fig. 2** Molecular structure of anion $\mathbf{3}^{2-}$ with displacement ellipsoids drawn at the 20% probability level. Only one position of the disordered silver atom is represented.

$$Pr(OTf)_3 + 6\,[PPh_4][NO_2] \xrightarrow[-\,[PPh_4][NO_2]\;-\,3\,[PPh_4][OTf]]{\text{pyridine}} [PPh_4]_2[Pr(\kappa^2\text{-}NO_2)_5(py)]\;([PPh_4]_2[\mathbf{4}]) \quad (5)$$

$$Nd(OTf)_3 + 6\,[PPh_4][NO_2] \xrightarrow[-\,[PPh_4][NO_2]\;-\,3\,[PPh_4][OTf]]{\text{pyridine}} [PPh_4]_2[Nd(\kappa^2\text{-}NO_2)_4(py)_2][NO_2]\;([PPh_4]_2[\mathbf{5}][NO_2]) \quad (6)$$

$$PrI_3 + 2\,[PPh_4][NO_2] + 3\,AgNO_2 \xrightarrow[-\,3\,AgI]{\text{pyridine}} [PPh_4]_2[\mathbf{4}] \quad (7)$$

$$NdI_3 + 2\,[PPh_4][NO_2] + 3\,AgNO_2 \xrightarrow[-\,3\,AgI]{\text{pyridine}} [PPh_4]_2[Nd(\kappa^2\text{-}NO_2)_5(py)]\;([PPh_4]_2[\mathbf{6}]) + [PPh_4]_2[Nd(\kappa^2\text{-}NO_2)_4(\kappa^1\text{-}NO_2)(py)]\;([PPh_4]_2[\mathbf{7}]) \quad (8)$$

$$LnI_3 + 3\,[PPh_4][NO_2] + 3\,AgNO_2 \xrightarrow[-\,[PPh_4][I]\;-\,2\,AgI]{\text{pyridine}} [PPh_4]_2[Ln(\kappa^2\text{-}NO_2)_4(\kappa^1\text{-}NO_2)_2Ag(py)_2]\;([PPh_4]_2[\mathbf{8}]\,(Pr)\;[PPh_4]_2[\mathbf{9}]\,(Nd)) \quad (9)$$

$$[PPh_4]_2[\mathbf{6}]\;[PPh_4]_2[\mathbf{7}] + AgNO_2 \xrightarrow{\text{pyridine}} [PPh_4]_2[\mathbf{9}] \quad (10)$$

**Scheme 2** Syntheses of $[PPh_4]_2[\mathbf{4}]$, $[PPh_4]_2[\mathbf{5}][NO_2]$, $[PPh_4]_2[\mathbf{6}]$, $[PPh_4]_2[\mathbf{7}]$, $[PPh_4]_2[\mathbf{8}]$ and $[PPh_4]_2[\mathbf{9}]$ by salt metathesis reactions, carried out at RT in pyridine solvent.

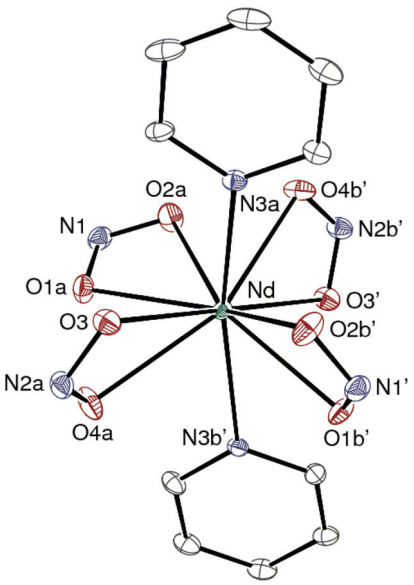


**Fig. 3** Molecular structure of anion $\mathbf{5}^{-}$ with displacement ellipsoids drawn at the 20% probability level. Only one set of positions of the disordered atoms is represented. Symmetry code: ′ = 1 − *x*, 1 − *y*, 1 − *z*.

also accessible with $Pr^{3+}$ and $Nd^{3+}$ ions and $[PPh_4]_2[Nd(\kappa^2\text{-}NO_2)_4(\kappa^1\text{-}NO_2)_2Ag(py)_2]$ (Ln = Pr ($[PPh_4]_2[\mathbf{8}]$), Nd $[PPh_4]_2[\mathbf{9}]$) were successfully formed according to eqn (9) and (10) (Scheme 2). $[PPh_4]_2[\mathbf{8}]$ and $[PPh_4]_2[\mathbf{9}]$ are isomorphous and differ from $[PPh_4]_2[\mathbf{3}]$ by the coordination modes of the six nitrite ligands. Indeed, both $\mathbf{8}^{2-}$ and $\mathbf{9}^{2-}$ feature four $\kappa^2$-(*O*,*O*) and two $\kappa^1$-(*O*) $NO_2$ ligands, with one monodentate nitrite serving as a bridging ligand with a $Ag(py)_2^+$ cation (Fig. 5). The decoordination of one O-donor when $Ce^{3+}$ is replaced by $Pr^{3+}$ or $Nd^{3+}$ is readily explained by the lanthanide contraction.[18] The coordination versatility of the nitrite anion was therefore explored with smaller REEs, namely samarium, ytterbium and yttrium.

The addition of 6 equiv. $[PPh_4][NO_2]$ to a pyridine solution of $Sm(OTf)_3$ affords crystals of $[PPh_4]_2[Sm(\kappa^2\text{-}NO_2)_5]$ ($[PPh_4]_2[\mathbf{10}]$), after diffusion of $Et_2O$ into the crude mixture (eqn (11) in Scheme 3). Crystals of $[PPh_4]_2[Yb(\kappa^2\text{-}NO_2)_5]$ ($[PPh_4]_2[\mathbf{11}]$) and $[PPh_4]_2[Y(\kappa^2\text{-}NO_2)_5]$ ($[PPh_4]_2[\mathbf{12}]$) were obtained similarly, from $Yb(OTf)_3$ and $Y(OTf)_3$, respectively, and the three complexes are isomorphous. As depicted in

 

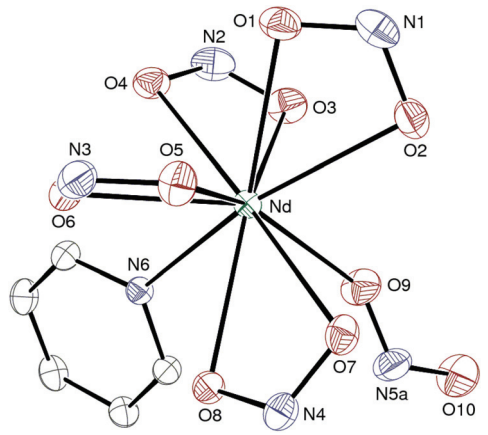


**Fig. 4** Molecular structure of anion $7^{2-}$ with displacement ellipsoids drawn at the 30% probability level. Only one position of the disordered atom is represented.

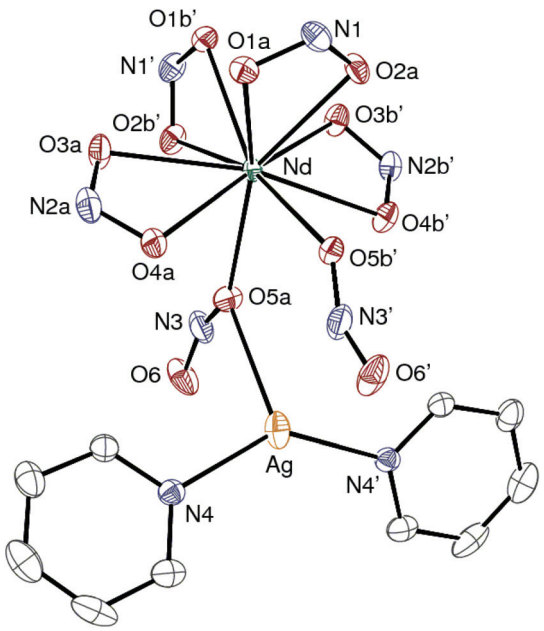


**Fig. 5** Molecular structure of anion $9^{2-}$ with displacement ellipsoids drawn at the 20% probability level. Only one set of positions of the disordered atoms is represented. Symmetry code: ′ = −*x*, *y*, 1/2 − *z*.

Fig. 6, $\mathbf{10}^{2-}$ is a pentanitrito complex of samarium(III) and the five nitrite ligands adopt the $\kappa^2$-(*O*,*O*)-$NO_2$ coordination mode. The distorted bicapped square antiprism in $\mathbf{10}^{2-}$ is better described by the distorted trigonal bipyramid defined by the $SmN_5$ backbone (Fig. 6) where N1, N2 and N3 form the equatorial plane. As such, $[PPh_4]_2$[**10**], $[PPh_4]_2$[**11**] and $[PPh_4]_2$[**12**] represent the first homoleptic nitrito complexes of the REEs. As discussed above, analytically pure samples of the complexes can be prepared in high yield using a combination of $[PPh_4][NO_2]$ and silver nitrite, as exemplified with the synthesis of $[PPh_4]_2$[**10**], from $SmI_3$, in eqn (12). Noticeably, utilization of $AgNO_2$ enables the formation of the hexanitrito complexes

$$Ln(OTf)_3 + 6\,[PPh_4][NO_2] \xrightarrow[-\,[PPh_4][NO_2]\;-\,3\,[PPh_4][OTf]]{\text{pyridine}} [PPh_4]_2[Ln(\kappa^2\text{-}NO_2)_5]\;([PPh_4]_2\mathbf{[10]}\;(Sm),\;[PPh_4]_2\mathbf{[11]}\;(Yb),\;[PPh_4]_2\mathbf{[12]}\;(Y)) \quad (11)$$

$$SmI_3 + 2\,[PPh_4][NO_2] + 3\,AgNO_2 \xrightarrow[-\,3\,AgI]{\text{pyridine}} [PPh_4]_2\mathbf{[10]} \quad (12)$$

$$LnI_3 + 3\,[PPh_4][NO_2] + 3\,AgNO_2 \xrightarrow[-\,[PPh_4][I]\;-\,2\,AgI]{\text{pyridine}} [PPh_4]_2[Ln(\kappa^2\text{-}NO_2)_3(\kappa^1\text{-}NO_2)_3Ag(py)_2]\;([PPh_4]_2\mathbf{[13]}\;(Sm),\;[PPh_4]_2\mathbf{[14]}\;(Y)) \quad (13)$$

$$[PPh_4]_2\mathbf{[10]} + AgNO_2 \xrightarrow{\text{pyridine}} [PPh_4]_2\mathbf{[13]} \quad (14)$$

$$SmI_2 + \text{xs}\;[PPh_4][NO_2] \xrightarrow[-\,[PPh_4][I]]{\text{pyridine}} [PPh_4]_2\mathbf{[10]} + \text{by-products} \quad (15)$$

**Scheme 3** Syntheses of $[PPh_4]_2$[**10**], $[PPh_4]_2$[**11**] and $[PPh_4]_2$[**12**] by salt metathesis reactions, carried out at RT in pyridine solvent.

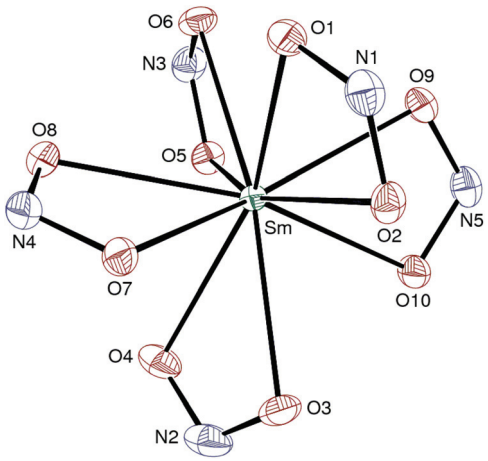


**Fig. 6** Molecular structure of anion $\mathbf{10}^{2-}$ with displacement ellipsoids drawn at the 20% probability level.

of samarium(III) and yttrium(III). In fact, $LnI_3$ (Ln = Sm, Y) reacts with a 3 : 3 mixture $[PPh_4][NO_2]$ and $AgNO_2$ to yield $[PPh_4]_2[Ln(\kappa^2\text{-}NO_2)_3(\kappa^1\text{-}NO_2)_3Ag(py)_2]$ (Ln = Sm ($[PPh_4]_2$[**13**]), Y ($[PPh_4]_2$[**14**])), at room temperature, and the purity of $[PPh_4]_2$[**13**] was confirmed by H, C, N elemental analyses (see the Experimental section). As shown in Fig. 7, anion $\mathbf{13}^{2-}$ results from the coordination of three $\kappa^2$-(*O*,*O*) and three $\kappa^1$-(*O*) $NO_2^-$ ligands to the $Sm^{3+}$ cation, in agreement with the smaller ionic radius of samarium (and yttrium), compared to neodymium. Interestingly, $[PPh_4]_2$[**13**] is obtained as a coordination polymer with the $[Ag(py)_2]^+$ cation bridging two $[Ln(\kappa^2\text{-}NO_2)_3(\kappa^1\text{-}NO_2)_3]^{3-}$ units *via* coordination to two $\kappa^1$-(*O*)-$NO_2$ ligands (Fig. 7). Overall, the formation of REEs/Ag complexes $[PPh_4]_2$[**X**] (**X** = **3**, **8**, **9**, **13**, **14**) demonstrates the potential of anionic Ln nitrito compounds to serve as building blocks for the synthesis of novel heterometallic coordination polymers.

As outlined in the introduction, the nitrite anion behaves as a one electron oxidant towards uranium(III) and uranium(IV) to yield a U=O functional group, with the concomitant release of NO.[4,12] Interestingly, cerium(III) complex $[PPh_4]_2$[**2**] is thermally stable and no oxidation of the metal ion to $Ce^{4+}$ was

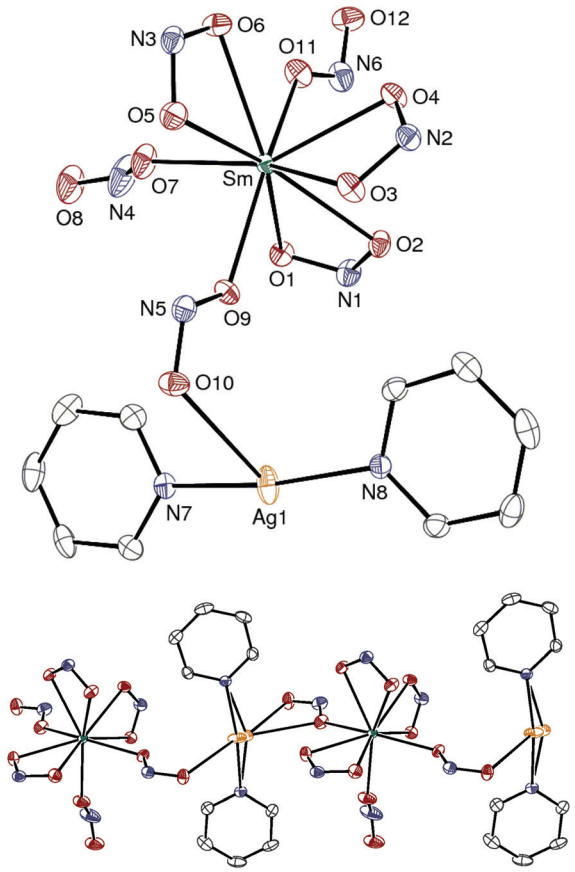


Fig. 7 Molecular structure of anion $\mathbf{13}^{2-}$ (top) and its polymeric organization (bottom) with displacement ellipsoids drawn at the 20% probability level. Only one position of the disordered silver atom is represented in the upper view.

observed upon heating a pyridine solution of the complex at 120 °C for 7 days. This stability likely originates from the rather high oxidation potential of $Ce^{3+}$.[19] In contrast, $Sm^{II}I_2$ is readily oxidized to $Sm^{III}$ in the presence of $[PPh_4][NO_2]$. In fact, the salt metathesis reaction between $SmI_2$ and 6 equiv. $[PPh_4][NO_2]$ results in slow gas evolution and the formation of crystals of $[PPh_4]_2[\mathbf{10}]$ and a white solid (eqn (15) in Scheme 3). Given the absence of the oxo group in $[PPh_4]_2[\mathbf{10}]$, the latter solid likely features an "$Sm_2O_3$" fragment.

Having in hand a series of 14 novel nitrito complexes of the rare earth elements, general trends can be deduced from their X-ray structures. First, in the absence of a Lewis acidic countercation, pentanitrito REEs complexes ($[PPh_4]_2[\mathbf{X}]$, **X** = **1**, **2**, **4**, **6**, **10**, **11**, **12**) are formed selectively across the series. The formation of hexanitrito complexes is available for all the elements and it requires the presence of $Ag^+$ as a cation, presumably to balance the electrostatic inter-ligand repulsion through coordination (as shown in $[PPh_4]_2[\mathbf{X}]$, **X** = **3**, **7**, **8**, **9**, **13**, **14**). Nonetheless, the coordination of the REE cation varies and it is directly controlled by the metal ionic radius. Following the lanthanide contraction, the pentanitrito complexes exhibit a coordination number of 11 for La–Nd and a coordination number of 10 for Nd–Y. $Nd^{3+}$ is the pivot in this series of complexes and four distinct structures were obtained with this single cation. The coordination sphere of the hexanitrito complexes is even more sensitive to the lanthanide contraction and, while $[PPh_4]_2[\mathbf{3}]$ (Ln = Ce) is undeca-coordinated, complexes $[PPh_4]_2[\mathbf{X}]$ (**X** = **8** (Pr), **9** (Nd)) are deca-coordinated and $[PPh_4]_2[\mathbf{13}]$ (Ln = Sm) and $[PPh_4]_2[\mathbf{14}]$ (Ln = Y) are nona-coordinated, resulting in a progressive increase in the number of $\kappa^1$-(*O*)-$NO_2$ ligands. The contraction is also observable in the linear decrease of the mean M–O bond distance measured for the M-[$\kappa^2$-(*O*,*O*)-$NO_2$] interactions (Table 1). In complexes $[PPh_4]_2[\mathbf{X}]$ (**X** = **3**, **6**, **8**, **9**, **13**, **14**), the nitrito ligands adopt two different coordination modes, namely $\kappa^2$-(*O*,*O*) and $\kappa^1$-(*O*), and we found that the M–O bond distance is ~0.16 Å shorter for the $\kappa^1$-(*O*)-bound nitrito ligand, regardless of the nature of the REE or the coordination of $Ag^I$. This finding is in agreement with the 0.15 Å bond difference observed in $[PPh_4]_2[UO_2(\kappa^2\text{-}NO_2)_2(\kappa^1\text{-}NO_2)_2]$.[4] However, all the nitrito complexes reported herein present a single set of two NO stretching frequencies in their IR spectra (1212–1229 and 1305–1307 $cm^{-1}$), including for complexes with two different nitrite coordination modes. In comparison, the nitrite anion is characterized by frequencies at 1240 and 1311 $cm^{-1}$ in $[PPh_4][NO_2]$ and at 1212 and 1304 $cm^{-1}$ in $[PPh_4]_2[Th(\kappa^2\text{-}NO_2)_6]$.[4]

In summary, the coordination chemistry of the nitrite anion has been investigated with rare earth elements, and the resulting complexes were structurally characterized. Among them, the first homoleptic examples of nitrite complexes of samarium, ytterbium and yttrium are described. The coordination behavior of the nitrite ion is directly controlled by the ionic radius of the metal cation. While the nitrito ligand is stable in the coordination sphere of cerium(III), it is readily reduced by $SmI_2$.

## Experimental section

### General considerations

The complexes described herein are all moisture sensitive. Syntheses and manipulations of the compounds were conducted under a ultra-high purity argon atmosphere with rigorous exclusion of air and water, using Schlenk-vessel and vacuum-line techniques or recirculating mBraun LabMaster glove boxes. Glassware was dried overnight at 120 °C before use. IR samples were prepared as Nujol mulls between KBr round cell windows and the spectra recorded on a Perkin-Elmer FT-IR 1725X spectrometer. Elemental analyses were performed at Medac Ltd at Chobham, Surrey (United Kingdom). Celite (Aldrich) and 4 Å molecular sieves (Aldrich) were dried under dynamic vacuum at 250 °C for 48 h prior to use. $PPh_4I$, $AgNO_2$ and the lanthanide precursors $SmI_2$, $Ln(OTf)_3$ (Ln = La, Ce, Pr, Nd, Sm, Yb, Y) and $LnI_3$ (Ln = Ce, Pr, Nd, Sm, Yb, Y) were purchased from commercial suppliers (Aldrich and Acros) and directly used without purification. $[PPh_4][NO_2]$ was synthesized as previously described.[4] Pyridine was dried over sodium and distilled before use. Tetrahydrofuran (THF), tetrahydrofuran-$d_8$ (THF-$d_8$), pentane, diethyl ether and benzene-$d_6$

 

were dried over a sodium(0)–benzophenone mixture and distilled before use. Acetonitrile, acetonitrile-$d_3$, dichloromethane and dichloromethane-$d_2$ were dried over $CaH_2$ and distilled before use.

### General procedure for the formation of crystals $[PPh_4]_2$[1], $[PPh_4]_2$[2], $[PPh_4]_2$[4], $[PPh_4]_2$[5], $[PPh_4]_2$[10], $[PPh_4]_2$[11] and $[PPh_4]_2$[12]

An NMR tube was charged with $Ln(OTf)_3$, 6 equiv. $[PPh_4][NO_2]$ and freshly distilled pyridine (~0.5 mL). After complete dissolution of the solids, the solution was sonicated in an ultrasonic bath for 1 h. Crystals were grown for days by slow diffusion of a blank of pure pyridine (0.1 mL) and then diethyl ether (1.5 mL) onto the initial mixture in pyridine. The quantities for the preparation of $[PPh_4]_2$[**1**], $[PPh_4]_2$[**2**], $[PPh_4]_2$[**4**], $[PPh_4]_2$[**5**], $[PPh_4]_2$[**10**], $[PPh_4]_2$[**11**] and $[PPh_4]_2$[**12**] were as follows:

- $[PPh_4]_2[La(\kappa^2\text{-}NO_2)_5(py)]$ ($[PPh_4]_2$[**1**]): $La(OTf)_3$ (22.2 mg, 0.038 mmol) and $[PPh_4][NO_2]$ (87.6 mg, 0.227 mmol). Translucent light yellow crystals were formed after 2 days.

- $[PPh_4]_2[Ce(\kappa^2\text{-}NO_2)_5(py)]$ ($[PPh_4]_2$[**2**]): $Ce(OTf)_3$ (29.4 mg, 0.050 mmol) and $[PPh_4][NO_2]$ (115.6 mg, 0.30 mmol). Translucent light yellow crystals were obtained after 1 day.

- $[PPh_4]_2[Pr(\kappa^2\text{-}NO_2)_5(py)]$ ($[PPh_4]_2$[**4**]): $Pr(OTf)_3$ (15.2 mg, 0.026 mmol) and $[PPh_4][NO_2]$ (59.8 mg, 0.155 mmol). Translucent light yellow crystals were obtained after 2 days.

- $[PPh_4]_2[Nd(\kappa^2\text{-}NO_2)_4(py)_2](NO_2)$ ($[PPh_4]_2$[**5**]): $Nd(OTf)_3$ (23.5 mg, 0.040 mmol) and $[PPh_4][NO_2]$ (91.9 mg, 0.239 mmol). Colourless crystals were obtained after 5 days.

- $[PPh_4]_2[Sm(\kappa^2\text{-}NO_2)_5]$ ($[PPh_4]_2$[**10**]): $Sm(OTf)_3$ (13.3 mg, 0.022 mmol) and $[PPh_4][NO_2]$ (51.6 mg, 0.134 mmol). Colourless crystals were obtained after 2 days.

- $[PPh_4]_2[Yb(\kappa^2\text{-}NO_2)_5]$ ($[PPh_4]_2$[**11**]): $Yb(OTf)_3$ (20.3 mg, 0.033 mmol) and$[PPh_4][NO_2]$ (75.7 mg, 0.196 mmol). Colourless crystals were obtained after 2 days.

- $[PPh_4]_2[Y(\kappa^2\text{-}NO_2)_5]$ ($[PPh_4]_2$[**12**]): $Y(OTf)_3$ (15.3 mg, 0.029 mmol) and $[PPh_4][NO_2]$ (66.0 mg, 0.171 mmol). Colourless crystals were obtained after two 2 days.

The synthesis, purification and elemental analyses for complexes $[PPh_4]_2$[**2**], $[PPh_4]_2$[**6**], $[PPh_4]_2$[**7**], $[PPh_4]_2$[**10**] are given thereafter, as representative examples. Data were not collected for compounds $[PPh_4]_2$[**1**], $[PPh_4]_2$[**4**], $[PPh_4]_2$[**5**], $[PPh_4]_2$[**11**] and $[PPh_4]_2$[**12**].

### Synthesis of $[PPh_4]_2[Ce(NO_2)_5(py)]$ ($[PPh_4]_2$[2])

A 25 mL round bottom flask was charged with $CeI_3$ (72.0 mg, 0.138 mmol), 2 equiv. $[PPh_4][NO_2]$ (106.6 mg, 0.276 mmol), 3 equiv. $AgNO_2$ (63.8 mg, 0.415 mmol) and freshly distilled pyridine (10 mL). After complete dissolution of the solids, the clear yellow solution, sheltered from light, was vigorously stirred at room temperature for 1 h. The solvent was then evaporated off and after 15 h drying under vacuum, acetonitrile (10 mL) was condensed onto the yellow residue. Rapidly, a pale-yellow precipitate of AgI deposited which was filtered off from the yellow solution. The solvent was then evaporated off and the residue was dried under vacuum (15 h, rt) to afford pure $[PPh_4]_2$[**2**] as a yellow powder (143.9 mg, 92%). Yellow crystals of $[PPh_4]_2$[**2**] were formed by slow diffusion of diethyl ether (1.5 mL) on a pyridine solution (0.5 mL) of the product (*ca.* 10 mg).

Anal. calcd for $C_{53}H_{45}CeN_6O_{10}P_2$ (1128.03): C, 56.43; H, 4.02; N, 7.45; Found: C, 56.12; H, 4.24; N, 7.54; IR ($cm^{-1}$): 525, 616, 688, 722, 754, 821, 850, 994, 1033, 1104, 1157, 1215 (N–O), 1305 (N–O), 1584, 2671, 2726.

### Synthesis of $[PPh_4]_2[Nd(NO_2)_5(py)]$ ($[PPh_4]_2$[6] and ($[PPh_4]_2$[7])

A 25 mL round bottom flask was charged with $NdI_3$ (83.7 mg, 0.159 mmol), 2 equiv. $[PPh_4][NO_2]$ (122.9 mg, 0.319 mmol), 3 $AgNO_2$ (73.6 mg, 0.478 mmol) and freshly distilled pyridine (10 mL). After complete dissolution of the solids, the solution, sheltered from light, was vigorously stirred at room temperature for 1 h. The solvent was then evaporated off and after 15 h drying under vacuum, the product was separated from the insoluble AgI by extraction in acetonitrile (10 mL). The solvent was then evaporated off and the residue dried under vacuum (15 h, rt) to afford pure $[PPh_4]_2[Nd(NO_2)_5(py)]$ as an off-white powder (169.2 mg, 94%). Colourless crystals of $[PPh_4]_2$[**6**] were formed by slow diffusion of diethyl ether (1.5 mL) on a pyridine solution (0.5 mL) of the product (*ca.* 10 mg). Colourless crystals of $[PPh_4]_2$[**7**] were obtained similarly but with diffusion of pentane instead of $Et_2O$.

Anal. calcd for $C_{53}H_{45}N_6NdO_{10}P_2$ (1132.15): C, 56.23; H, 4.01; N, 7.42; Found: C, 55.77; H, 3.84; N, 7.46. IR ($cm^{-1}$): 524, 617, 688, 722, 754, 823, 994, 1021, 1101, 1156, 1221 (N–O), 1305 (N–O), 1584, 2671, 2726.

### Synthesis of $[PPh_4]_2[Sm(NO_2)_5]$ ($[PPh_4]_2$[10])

A 25 mL round bottom flask was charged with $SmI_3$ (78.7 mg, 0.148 mmol), 2 equiv. $[PPh_4][NO_2]$ (114.2 mg, 0.296 mmol), 3 equiv. $AgNO_2$ (68.4 mg, 0.444 mmol) and freshly distilled pyridine (10 mL). After complete dissolution of the solids, the solution, sheltered from light, was vigorously stirred at room temperature for 1 h. The solvent was then evaporated off and after 15 h drying under vacuum, the product was separated from the insoluble AgI by extraction in acetonitrile (10 mL). The solvent was then evaporated off and the leaving off-white powder was dried under vacuum for 15 h to afford $[PPh_4]_2$[**10**] in almost quantitative yield (156.1 mg). Colourless crystals of $[PPh_4]_2$[**10**] were grown by slow diffusion of diethyl ether (1.5 mL) on a pyridine solution (0.5 mL) of the product (*ca.* 10 mg).

Anal. calcd for $C_{48}H_{40}N_5O_{10}P_2Sm$ (1059.17): C, 54.43; H, 3.81; N, 6.61; found: C, 55.16; H, 3.78; N, 6.87; the analysis suggests that the compound is not completely desolvated and would contain 0.4 pyridine (required C, 55.05; H, 3.88; N, 6.93). IR ($cm^{-1}$): 527, 617, 688, 722, 751, 826, 850, 891, 968, 996, 1025, 1104, 1158, 1229 (N–O), 1305 (N–O), 1584, 2671, 2726.

### General procedure for the preparation of the crystals of $[PPh_4]_2$[3], $[PPh_4]_2$[8], $[PPh_4]_2$[9], $[PPh_4]_2$[13] and $[PPh_4]_2$[14] containing silver salt

An NMR tube was charged with $LnI_3$, 3.0 equiv. $[PPh_4][NO_2]$, 3.0 equiv. $AgNO_2$ and freshly distilled pyridine (~0.5 mL). After

complete dissolution, the solution sheltered from light was sonicated in an ultrasonic bath for 1 h. Crystals were grown for days by slow diffusion of pyridine (0.1 mL) and then diethyl ether (1.5 mL) on the initial pyridine mixture. The quantities for the preparation of $[PPh_4]_2$[**3**], $[PPh_4]_2$[**8**], $[PPh_4]_2$[**9**], $[PPh_4]_2$[**13**] and $[PPh_4]_2$[**14**] were as follow:

- $[PPh_4]_2[Ce(\kappa^2\text{-}NO_2)_5(\kappa^1\text{-}NO_2)Ag(py)_2]$ ($[PPh_4]_2$[**3**]): $CeI_3$ (12.1 mg, 0.023 mmol), $[PPh_4][NO_2]$ (27.0 mg, 0.07 mmol) and $AgNO_2$ (11.0 mg, 0.07 mmol). Translucent light yellow crystals were obtained after 3 days.

- $[PPh_4]_2[Pr(\kappa^2\text{-}NO_2)_5(\kappa^1\text{-}NO_2)Ag(py)_2]$ ($[PPh_4]_2$[**8**]): $PrI_3$ (16.5 mg, 0.032 mmol), $[PPh_4][NO_2]$ (36.6 mg, 0.095 mmol) and $AgNO_2$ (14.6 mg, 0.095 mmol). Translucent light yellow crystals were obtained after 2 days.

- $[PPh_4]_2[Nd(\kappa^2\text{-}NO_2)_4(\kappa^1\text{-}NO_2)_2Ag(py)_2]$ ($[PPh_4]_2$[**9**]): $NdI_3$ (17.8 mg, 0.034 mmol), $[PPh_4][NO_2]$ (39.3 mg, 0.10 mmol) and $AgNO_2$ (15.7 mg, 0.102 mmol). Colourless crystals were obtained after 3 days.

- $[PPh_4]_2[Sm(\kappa^2\text{-}NO_2)_3(\kappa^1\text{-}NO_2)_3Ag(py)_2]$ ($[PPh_4]_2$[**13**]): $SmI_3$ (16.2 mg, 0.03 mmol), $[PPh_4][NO_2]$ (35.2 mg, 0.091 mmol) and $AgNO_2$ (14.1 mg, 0.091 mmol). Colourless crystals were obtained after 3 days.

- $[PPh_4]_2[Y(\kappa^2\text{-}NO_2)_3(\kappa^1\text{-}NO_2)_3Ag(py)_2]$ ($[PPh_4]_2$[**14**]): $YI_3$ (15.9 mg, 0.034 mmol), $[PPh_4][NO_2]$ (39.3 mg, 0.102 mmol) and $AgNO_2$ (15.7 mg, 0.10 mmol). Colourless crystals were obtained after 3 days.

The synthesis, purification and elemental analyses for complexes $[PPh_4]_2$[**3**] and $[PPh_4]_2$[**13**] are given thereafter, as representative examples. Data were not collected for compounds $[PPh_4]_2$[**8**], $[PPh_4]_2$[**9**] and $[PPh_4]_2$[**14**].

### Synthesis of $[PPh_4]_2[Ce(NO_2)_6Ag(py)_{1.5}]$ and crystals of $[PPh_4]_2$[3]

A 25 mL round bottom flask was charged with $[PPh_4]_2$[**2**] (35.8 mg, 0.032 mmol), 1 equiv. $AgNO_2$ (4.9 mg, 0.003 mmol) and freshly distilled pyridine (5 mL). After complete dissolution of the solids, the yellow solution, sheltered from light, was vigorously stirred at room temperature for 1 h. The solvent was then evaporated off and after 15 h under vacuum, a yellow brown powder of a product $[PPh_4]_2[Ce(NO_2)_6Ag(py)_{1.5}]$ was isolated (40.8 mg, 97%). Translucent light yellow crystals of $[PPh_4]_2$[**3**] were grown by slow diffusion of diethyl ether (1.5 mL) in a pyridine solution (0.5 mL) of the analyzed product (*ca.* 10 mg).

Anal. calcd for $C_{55.5}H_{47.5}AgCeN_{7.5}O_{12}P_2$ (1321.45): C, 50.44; H, 3.62; N, 7.95; Found: C, 49.73; H, 3.64; N, 8.35; IR ($cm^{-1}$): 524, 689, 705, 722, 757, 800, 824, 891, 995, 1106, 1156, 1212 (N–O), 1305 (N–O), 1584, 1599, 2671, 2726.

### Synthesis of $[PPh_4]_2[Sm(NO_2)_6Ag(py)_2]$ ($[PPh_4]_2$[13])

A 25 mL round bottom flask was charged with $[PPh_4]_2$[**10**] (52.3 mg, 0.049 mmol), 3 equiv. $AgNO_2$ (7.6 mg, 0.005 mmol.) and freshly distilled pyridine (5 mL). After complete dissolution of the solids, the solution, sheltered from light, was vigorously stirred at room temperature for 1 h. The solvent was then evaporated off and after 15 h under vacuum, $[PPh_4]_2$[**13**] was isolated pure as a pale brown powder (65.1 mg, 96%). Colourless crystals of $[PPh_4]_2$[**13**] were grown by slow diffusion of diethyl ether (1.5 mL) on a pyridine solution (0.5 mL) of the product (*ca.* 10 mg).

Anal. calcd for $C_{58}H_{50}AgN_8O_{12}P_2Sm$ (1371.24): C, 50.80; H, 3.68; N, 8.17; found: C, 50.86; H, 3.79; N, 8.38; IR ($cm^{-1}$): 523, 687, 722, 756, 803, 826, 1020, 1100, 1156, 1212 (N–O), 1261, 1307 (N–O), 1583, 1599, 2671, 2727.

### Oxidation of $Sm^{II}$ to $Sm^{III}$ by $[PPh_4][NO_2]$

An NMR tube was charged with $SmI_2$ (17.8 mg, 0.04 mmol) and a solution of 6 equiv. $[PPh_4][NO_2]$ (101.8 mg, 0.26 mmol) and freshly distilled pyridine (~0.5 mL). The mixture was then sonicated for 1 h, a time during which the black insoluble $SmI_2$ was transformed into a white precipitate with a few but visible release of gas. The solution was then filtered-off and crystals were grown by slow diffusion of diethyl ether (1.5 mL) on the pyridine filtrate. Colourless crystals of $[PPh_4]_2[Sm(NO_2)_5]$ ($[PPh_4]_2$[**10**]) were obtained after 3 days.

### Crystallography

The data were collected at 150(2) K on a Nonius Kappa-CCD area detector diffractometer[20] using graphite-monochromated MoKα radiation ($\lambda$ = 0.71073 Å). The crystals were introduced into glass capillaries with a protecting "Paratone-N" oil (Hampton Research) coating. The unit cell parameters were determined from ten frames, then refined on all data. The data (combinations of φ- and ω-scans with a minimum redundancy of 4 for 90% of the reflections) were processed with HKL2000.[21] Absorption effects were corrected empirically with the program SCALEPACK.[21] The structures were solved by direct methods with SHELXS-97, expanded by subsequent Fourier-difference synthesis and refined by full-matrix least-squares on $F^2$ with SHELXL-97.[22] All non-hydrogen atoms were refined with anisotropic displacement parameters. The hydrogen atoms were introduced at calculated positions and were treated as riding atoms with an isotropic displacement parameter equal to 1.2 times that of the parent atom. Special details are as follows.

In the series of isomorphous complexes $[PPh_4]_2$[**1**], $[PPh_4]_2$[**2**], $[PPh_4]_2$[**4**] and $[PPh_4]_2$[**6**], two nitrite ions (containing N1 and N5) are badly resolved. In all cases, one of them (N5) was found to be disordered over two positions sharing the oxygen atom O10, which were refined with occupancy parameters constrained to sum to unity. In complex $[PPh_4]_2$[**6**] only, the nitrite containing N1 could also be modeled with two positions; the position A of the nitrite containing N1 and B of that containing N5 are incompatible, and the occupancy parameters, constrained to sum to unity, have been assigned accordingly. Restraints on bond lengths, angles and displacement parameters had to be applied for several nitrite ions in all these compounds.

In complexes $[PPh_4]_2$[**3**], $[PPh_4]_2$[**13**] and $[PPh_4]_2$[**14**], the Ag atom is disordered over two positions which were refined with occupancy parameters constrained to sum to unity.

 

**Table 2** Crystal data and structure refinement details

| | $[PPh_4]_2$[**1**] | $[PPh_4]_2$[**2**] | $[PPh_4]_2$[**3**] | $[PPh_4]_2$[**4**] | $[PPh_4]_2$[**5**][$NO_2$] | $[PPh_4]_2$[**6**] | $[PPh_4]_2$[**7**] |
|---|---|---|---|---|---|---|---|
| Chemical formula | $C_{53}H_{45}LaN_6O_{10}P_2$ | $C_{53}H_{45}CeN_6O_{10}P_2$ | $C_{58}H_{50}AgCeN_8O_{12}P_2$ | $C_{53}H_{45}N_6O_{10}P_2Pr$ | $C_{58}H_{50}N_7NdO_{10}P_2$ | $C_{53}H_{45}N_6NdO_{10}P_2$ | $C_{53}H_{45}N_6NdO_{10}P_2$ |
| $M$/g mol$^{-1}$ | 1126.80 | 1128.01 | 1360.99 | 1128.80 | 1211.23 | 1132.13 | 1132.13 |
| Crystal system | Monoclinic | Monoclinic | Triclinic | Monoclinic | Triclinic | Monoclinic | Triclinic |
| Space group | $P2_1/c$ | $P2_1/c$ | $P\bar{1}$ | $P2_1/c$ | $P\bar{1}$ | $P2_1/c$ | $P\bar{1}$ |
| $a$/Å | 13.2741(4) | 13.2645(5) | 10.3567(5) | 13.2497(4) | 9.4292(2) | 13.2408(2) | 10.0031(4) |
| $b$/Å | 17.9504(8) | 17.9358(7) | 16.1781(9) | 17.9467(6) | 9.6856(3) | 17.9735(4) | 12.8890(7) |
| $c$/Å | 21.7777(8) | 21.7448(7) | 17.3706(6) | 21.7355(3) | 15.8367(6) | 21.7067(3) | 21.3346(11) |
| $\alpha$/° | 90 | 90 | 97.503(4) | 90 | 76.145(2) | 90 | 87.813(2) |
| $\beta$/° | 96.307(3) | 96.433(2) | 97.694(4) | 96.6330(18) | 75.304(2) | 96.8113(12) | 77.576(3) |
| $\gamma$/° | 90 | 90 | 98.777(3) | 90 | 81.595(2) | 90 | 68.306(3) |
| $V$/Å$^3$ | 5157.7(3) | 5140.7(3) | 2816.4(2) | 5133.9(2) | 1352.68(7) | 5129.38(16) | 2493.4(2) |
| $Z$ | 4 | 4 | 2 | 4 | 1 | 4 | 2 |
| $D_{calc}$/g cm$^{-3}$ | 1.451 | 1.457 | 1.605 | 1.460 | 1.487 | 1.466 | 1.508 |
| $\mu$(MoKα)/mm$^{-1}$ | 0.954 | 1.012 | 1.273 | 1.075 | 1.085 | 1.139 | 1.171 |
| $F$(000) | 2288 | 2292 | 1370 | 2296 | 617 | 2300 | 1150 |
| Reflections collected | 17 4882 | 176 769 | 141 359 | 193 839 | 80 560 | 191 378 | 159 280 |
| Independent reflections | 9781 | 9748 | 10 682 | 9732 | 8246 | 15 604 | 15 217 |
| Observed reflections [$I > 2\sigma(I)$] | 7431 | 7415 | 7439 | 8308 | 7975 | 13 465 | 12 029 |
| $R_{int}$ | 0.045 | 0.049 | 0.072 | 0.025 | 0.037 | 0.018 | 0.051 |
| Parameters refined | 668 | 668 | 749 | 668 | 436 | 695 | 659 |
| $R_1$ | 0.057 | 0.058 | 0.049 | 0.057 | 0.028 | 0.040 | 0.033 |
| w$R_2$ | 0.161 | 0.160 | 0.129 | 0.165 | 0.076 | 0.112 | 0.069 |
| $S$ | 1.129 | 1.127 | 1.011 | 1.046 | 1.050 | 1.124 | 1.003 |
| $\Delta\rho_{min}$/e Å$^{-3}$ | −2.05 | −1.51 | −1.01 | −1.66 | −1.03 | −1.19 | −1.05 |
| $\Delta\rho_{max}$/e Å$^{-3}$ | 1.76 | 2.17 | 1.39 | 3.31 | 0.77 | 2.11 | 0.56 |

| | $[PPh_4]_2$[**8**] | $[PPh_4]_2$[**9**] | $[PPh_4]_2$[**10**]·py | $[PPh_4]_2$[**11**]·py | $[PPh_4]_2$[**12**]·py | $[PPh_4]_2$[**13**] | $[PPh_4]_2$[**14**] |
|---|---|---|---|---|---|---|---|
| Chemical formula | $C_{58}H_{50}AgN_8O_{12}P_2Pr$ | $C_{58}H_{50}AgN_8NdO_{12}P_2$ | $C_{53}H_{45}N_6O_{10}P_2Sm$ | $C_{53}H_{45}N_6O_{10}P_2Yb$ | $C_{53}H_{45}N_6O_{10}P_2Y$ | $C_{58}H_{50}AgN_8O_{12}P_2Sm$ | $C_{58}H_{50}AgN_8O_{12}P_2Y$ |
| $M$/g mol$^{-1}$ | 1361.78 | 1365.11 | 1138.24 | 1160.93 | 1076.80 | 1371.22 | 1309.78 |
| Crystal system | Monoclinic | Monoclinic | Monoclinic | Monoclinic | Monoclinic | Triclinic | Triclinic |
| Space group | $C2/c$ | $C2/c$ | $P2_1/c$ | $P2_1/c$ | $P2_1/c$ | $P\bar{1}$ | $P\bar{1}$ |
| $a$/Å | 31.9249(10) | 31.8726(10) | 17.8243(8) | 17.7881(5) | 17.8054(7) | 10.1729(5) | 10.1741(3) |
| $b$/Å | 10.8245(5) | 10.8359(3) | 13.6518(3) | 13.6149(4) | 13.6258(6) | 11.6627(5) | 11.6470(5) |
| $c$/Å | 20.8700(8) | 20.8434(7) | 22.0678(10) | 21.9841(5) | 22.0104(5) | 24.7799(9) | 24.6852(12) |
| $\alpha$/° | 90 | 90 | 90 | 90 | 90 | 95.368(3) | 95.277(2) |
| $\beta$/° | 127.881(2) | 127.829(2) | 109.511(2) | 109.6818(17) | 109.628(2) | 93.817(3) | 94.020(3) |
| $\gamma$/° | 90 | 90 | 90 | 90 | 90 | 103.994(2) | 103.847(3) |
| $V$/Å$^3$ | 5692.4(4) | 5685.8(3) | 5061.5(3) | 5013.1(2) | 5029.7(3) | 2828.1(2) | 2815.2(2) |
| $Z$ | 4 | 4 | 4 | 4 | 4 | 2 | 2 |
| $D_{calc}$/g cm$^{-3}$ | 1.589 | 1.595 | 1.494 | 1.538 | 1.422 | 1.610 | 1.545 |
| $\mu$(MoKα)/mm$^{-1}$ | 1.316 | 1.374 | 1.288 | 1.995 | 1.288 | 1.501 | 1.501 |
| $F$(000) | 2744 | 2748 | 2308 | 2340 | 2216 | 1378 | 1332 |
| Reflections collected | 100 289 | 64 608 | 175 865 | 172 017 | 164 062 | 155 212 | 163 001 |
| Independent reflections | 8682 | 8658 | 13 075 | 15 284 | 12 979 | 17 283 | 17 198 |
| Observed reflections [$I > 2\sigma(I)$] | 6727 | 7081 | 8465 | 11 714 | 8570 | 12 818 | 11 391 |
| $R_{int}$ | 0.035 | 0.032 | 0.083 | 0.036 | 0.052 | 0.053 | 0.054 |
| Parameters refined | 425 | 425 | 649 | 649 | 649 | 749 | 749 |
| $R_1$ | 0.038 | 0.035 | 0.038 | 0.028 | 0.040 | 0.035 | 0.038 |
| w$R_2$ | 0.096 | 0.090 | 0.070 | 0.062 | 0.084 | 0.078 | 0.089 |
| $S$ | 1.135 | 1.168 | 0.911 | 0.955 | 0.961 | 0.982 | 1.002 |
| $\Delta\rho_{min}$/e Å$^{-3}$ | −1.74 | −1.95 | −0.88 | −1.03 | −0.46 | −1.08 | −0.56 |
| $\Delta\rho_{max}$/e Å$^{-3}$ | 1.94 | 1.62 | 0.66 | 0.50 | 0.35 | 1.08 | 0.92 |

In complex $[PPh_4]_2$[**5**][$NO_2$], all the nitrite ions, both coordinated and free, and the pyridine ligand, are disordered over two positions (sharing one nitrogen atom for one nitrite ion and one oxygen atom for another one), which have been refined with occupancy parameters constrained to sum to unity (fixed to 0.5 for the free nitrite which is disordered around an inversion centre). Restraints on bond lengths and displacement parameters had to be applied for the free nitrite anion, and the two positions of the pyridine molecule, close to one another, were refined as idealized hexagons.

In complex $[PPh_4]_2$[**7**], atom N5 is disordered over two positions which were refined with occupancy parameters constrained to sum to unity and with restraints on displacement parameters.

In the two isomorphous complexes $[PPh_4]_2$[**8**] and $[PPh_4]_2$[**9**], the three nitrite ions are disordered: two of them (containing N1 and N2) have two components nearly orthogonal to one another while only one oxygen atom is disordered over two positions in the third (N3). The occupancy parameters of all these positions have been refined to values very close to 0.5, then fixed to this value to allow for the mixing of the different positions and their symmetry equivalents (some positions being mutually incompatible). Restraints have been applied for some bond lengths and displacement parameters in the disordered parts.

Crystal data and structure refinement parameters are given in Table 2 and selected bond lengths and angles in Table 1. The molecular plots were drawn with ORTEP-3.[23]

## Acknowledgements

For financial support of this work, we acknowledge CEA, CNRS and ANR (Starting Grant to T. C.). T. C. thanks the Fondation Louis D. – Institut de France for its formidable support.

## Notes and references

1 (*a*) W. Runde and M. P. Neu, in *The Chemistry of the Actinide and Transactinide Elements*, ed. L. R. Morss, N. M. Edelstein and J. Fuger, Springer, Dordrecht, The Netherlands, 3rd edn, 2006, vol. 6, pp. 3475–3593; (*b*) K. L. Nash, C. Madic, J. N. Mathur and J. Lacquement, in *The Chemistry of the Actinide and Transactinide Elements*, ed. L. R. Morss, N. M. Edelstein and J. Fuger, Springer, Dordrecht, The Netherlands, 3rd edn, 2006, vol. 4, pp. 2622–2798; (*c*) M. S. Milyukova, N. S. Varezhkina and B. F. Myasoedov, *J. Radioanal. Nucl. Chem.*, 1986, **105**, 249–256; (*d*) A. Turanov, V. Karandashev and V. Baulin, *Solvent Extr. Ion Exch.*, 1999, **17**, 1423–1444; (*e*) A. Turanov, V. Karandashev, A. Kharitonov, A. Yarkevich and Z. Safronova, *Solvent Extr. Ion Exch.*, 2000, **18**, 1109–1134; (*f*) A. Turanov, V. Karandashev and A. Yarkevich, *Solvent Extr. Ion Exch.*, 2002, **20**, 1–19.

2 (*a*) *Rare Earth Elements: A Review of Production, Processing, Recycling, and Associated Environmental Issues*, US environmental protection agency, 600/R-12/572, December 2012, http://www.epa.gov/ord; (*b*) D. Schüler, M. Buchert, R. Liu, S. Dittrich and C. Merz, *Final Report for The Greens/EFA Group in the European Parliament*, Darmstadt, 2011.

3 (*a*) J. M. Mckibben, D. F. Chostner and E. G. Orebaugh, *Plutonium-uranium separation in the Purex process using mixtures of hydroxylamine nitrate and ferrous sulfamate*, E. I. du Pont de Nemours & co., Savannah River Laboratory, Aiken, South Carolina, United states of America, 1983; (*b*) R. J. W. Streeton and E. N. Jenkins, *The Preparation, Stabilisation and Analysis of Uranium(IV) Nitrate Solutions*, United Kingdom Atomic Energy Authority. Research Group. Atomic Energy Research Establishment, Harwell, Berks, England (United Kingdom), 1962; (*c*) C. S. Schlea, M. R. Caverly, H. E. Henry and W. J. Jenkins, *Uranium(IV) nitrate as a reducing agent for plutonium(IV) in the Purex process*, E. I. du Pont de Nemours & co., Savannah River Laboratory, Aiken, South Carolina, United states of America, 1963.

4 F. Dulong, J. Pouessel, P. Thuery, J. C. Berthet, M. Ephritikhine and T. Cantat, *Chem. Commun.*, 2013, **49**, 2412–2414.

5 (*a*) J. C. Barnes and R. D. Peacock, *J. Chem. Soc. A*, 1971, 558–562; (*b*) A. V. Kirschner, T. Luxbacher, H. P. Fritzer, B. Koppelhuber-Bitschnau, B. Nissen and C. D. Flint, *Spectrochim. Acta, Part A*, 1998, **54**, 2045–2049; (*c*) W. Y. Li and P. A. Tanner, *Inorg. Chem.*, 2010, **49**, 6384–6386.

6 Q.-Q. Kang, L.-S. Long, R.-B. Huang and L.-S. Zheng, *Acta Crystallogr., Sect. E: Struct. Rep. Online*, 2004, **60**, i12–i14.

7 G. H. Maunder, M. R. Russo and A. Sella, *Polyhedron*, 2004, **23**, 2709–2714.

8 W. Zhongzhi, X. Zheng, Y. Xiaozeng, W. Huaqing, Z. Xigen, S. Furen and H. Jiping, *J. Organomet. Chem.*, 1993, **455**, 93–97.

9 C. C. Ji, J. Li, Y. Z. Li, Z. J. Guo and H. G. Zheng, *CrystEngComm*, 2010, **12**, 3183–3194.

10 M. Diallo, M. Diop, P. M. Haba, M. Gaye, A. S. Sall, A. H. Barry, C. Beghidja and R. Welter, *J. Chem. Crystallogr.*, 2008, **38**, 475–478.

11 Q.-H. Zhao, Q.-H. Wang and R.-B. Fang, *Transition Met. Chem.*, 2004, **29**, 144–148.

12 A. J. Lewis, P. J. Carroll and E. J. Schelter, *J. Am. Chem. Soc.*, 2013, **135**, 511–518.

13 (*a*) M. A. Hitchman and G. L. Rowbottom, *Coord. Chem. Rev.*, 1982, **42**, 55–132; (*b*) R. D. Feltham, *Pure Appl. Chem.*, 1989, **61**, 943–946.

14 A. O. Borodin, G. A. Kostin, P. E. Plusnin, E. Y. Filatov, A. S. Bogomyakov and N. V. Kuratieva, *Eur. J. Inorg. Chem.*, 2012, **2012**, 2298–2304.

15 S. Khanjani, A. Morsali and P. Retailleau, *CrystEngComm*, 2010, **12**, 2173–2178.

16 (*a*) M. Wang, B. Wang, P. Zheng, W. Wang and J. Lin, *Acta Crystallogr., Sect. C: Cryst. Struct. Commun.*, 1988, **44**,

 

1913–1916; (*b*) J.-Y. Cheng, Y.-B. Dong, J.-P. Ma, R.-Q. Huang and M. D. Smith, *Inorg. Chem. Commun.*, 2005, **8**, 6–8.
17 (*a*) G. Paolucci, G. Marangoni, G. Bandoli and D. A. Clemente, *J. Chem. Soc., Dalton Trans.*, 1980, 459–466; (*b*) A. E. Bradley, C. Hardacre, M. Nieuwenhuyzen, W. R. Pitner, D. Sanders, K. R. Seddon and R. C. Thied, *Inorg. Chem.*, 2004, **43**, 2503–2514.
18 R. D. Shannon, *Acta Crystallogr., Sect. A: Cryst. Phys., Diffr., Theor. Gen. Cryst.*, 1976, **32**, 751–767.
19 N. A. Piro, J. R. Robinson, P. J. Walsh and E. J. Schelter, *Coord. Chem. Rev.*, 2014, **260**, 21–36.
20 R. W. W. Hooft, *COLLECT*, Nonius BV, Delft, The Netherlands, 1998.
21 Z. Otwinowski and W. Minor, *Methods Enzymol.*, 1997, **276**, 307–326.
22 G. M. Sheldrick, *Acta Crystallogr., Sect. A: Found. Crystallogr.*, 2008, **64**, 112–122.
23 L. J. Farrugia, *J. Appl. Crystallogr.*, 1997, **30**, 565.